Published in final edited form as:
Nanotechnology. 2011 March 11; 22(10): 105708. doi:10.1088/0957-4484/22/10/105708.

The role of surface charge on the uptake and biocompatibility of hydroxyapatite nanoparticles with osteoblast cells

Liang Chen[1], **Joseph M. Mccrate**[1,2], **James C-M. Lee**[3], and **Hao Li**[1,*]

[1]Department of Mechanical and Aerospace Engineering, University of Missouri, Columbia, MO 65203

[2]Department of Chemical Engineering, University of Texas at Austin, Austin, TX 78712

[3]Department of Biological Engineering, University of Missouri, Columbia, MO 65203

Abstract

The objective of this study is to evaluate the effect of hydroxyapatite (HAP) nanoparticles with different surface charges on the cellular uptake behavior and *in vitro* cell viability and proliferation of MC3T3-E1 cell lines (osteoblast). The nanoparticles surface charge was varied by the surface modification with two carboxylic acids: 12-aminododecanoic acid (positive) and dodecanedioic acid (negative). The untreated HAP nanoparticles and dodecanoic acid modified HAP nanoparticles (neutral) were used as the control. X-ray diffraction (XRD) revealed that surface modifications by the three carboxylic acids did not change the crystal structure of HAP nanoparticles; Fourier transform infrared spectroscopy (FTIR) confirmed the adsorption and binding of the carboxylic acids on HAP nanoparticle surface; and zeta potential measurement confirmed that the chemicals successfully modified the surface charge of HAP nanoparticles in water based solution. Transmission electron microscopy (TEM) images showed that positively charged, negatively charged and untreated HAP nanoparticles, with similar size and shape, all penetrated into the cells and cells had more uptake of HAP nanoparticles with positive charge compared to those with negative charge, which might be attributed to the attractive or repulsive interaction between the negatively charged cell membrane and positively/negatively charged HAP nanoparticles. The neutral HAP nanoparticles could not penetrate cell membrane due to the larger size. MTT assay and LDH assay results indicated that as compared with the polystyrene control, greater cell viability and cell proliferation were measured on MC3T3-E1 cells treated with the three kinds of the HAP nanoparticles (neutral, positive, and untreated), among which positively charged HAP nanoparticles shows strongest improvement for cell viability and cell proliferation. In summary, the surface charge of HAP nanoparticles can be modified to influence the cellular uptake of HAP nanoparticles and the different uptake also influence the behavior of cells. These *in-vitro* results may also provide useful information for investigations of HAP nanoparticles applications in the gene delivery and intracellular drug delivery.

1. Introduction

With unique physical, chemical, and biological properties, nanoparticles, with diameter in the 1 to 100 nm range, have been used in numerous physical, biomedical, and pharmaceutical fields [1–4]. There exist great interests in applications and environmental and health impact of variety of nanomaterials, such as carbon nanotubes[5], silica nanoparticles[6], fullerene[7, 8], magnetic nanoparticles[9], etc. Particularly, nanoparticles are believed to have the potential to assist in delivering drugs or genetic materials to targeted

*: liha@missouri.edu.

cells or organs and make the therapeutic delivery procedures more precise, more effective, and less harmful to healthy tissues and organs[10]. Most of current research on drug and gene delivery using nanomaterials focus on polymer nanoparticles, such as polyethylenimine (PEI)[11], chitosan [12], polyglycolic acid (PLGA) [13–15]. Metal and ceramic nanoparticles, such as Au nanoparticles [16–18], iron oxide [17, 19, 20], and silica nanoparticles [10, 21, 22] have also been studied for drug and gene delivery.

Hydroxyapatite(HAP), the primary inorganic component of bone and teeth, has been widely used in many biomedical fields such as dental composite [23], bone tissue engineering [9], orthopaedic implants [24, 25] and antibacterial agents [26] for its chemical and structural similarity with bone minerals and good biocompatibility. Recently, more efforts have been made to explore the potential of using HAP nanoparticles as vehicles for drug and gene delivery for their great affinity to DNA and various drugs and good release property[2, 10, 27–29]. Because gene delivery and intracellular drug delivery using HAP nanoparticles are dependent on cellular uptake, the understanding of the interaction of HAP nanoparticles with cells is critical for fundamental design of the nanoparticles for these gene delivery and drug delivery applications [30]. It is well known that size, shape, and surface charge are the primary parameters of colloidal particles for cellular uptake besides the biomolecular approach, such as using peptide. Motskin et al. recently reported that less negatively charged (closer to neutral) and rod-like HAP nanoparticles have an appreciable advantage over the spherical shape nanoparticles in terms of cellular uptake[31]. Gao et al. [32] proposed a theoretical model on receptor-mediated endocytosis process and gave an optimal radius of ~27–30nm for spherical particles for highest cellular uptake, which is in good agreement with many cellular uptake experimental results. Tang et al. [33] synthesized a series of spherical HAP nanoparticles with well defined sizes and revealed that, in both mesenchymal stem cells (MSC) and osteosarcoma cells (U2OS), the amount of uptaken HAP nanoparitcles decreased with the increase in particle size. Besides cellular uptake, the toxicity of nanoparticles has to be investigated for gene or drug delivery applications as well. Previous studies have shown that the HAP nanoparticles, normally a non-toxic material, can also cause cell damage *in vitro* similar as other nanomaterials [29, 34, 35]. It was found that spherical HAP nanoparticles showed favorable biocompatibility than rod-like HAP nanoparticles for osteoblasts [36]. Tang's paper reported that [33] the HAP nanoparticles have adverse effect on cell proliferation for MSC and U_2OS cells and the particle size also plays an important role on the cell proliferation process. All the previous studies indicates that a better understanding of the effects of surface charge on cellular uptake and biocompatibility of HAP nanoparticles is very helpful for the fundamental design of HAP nanoparticles for biomedical application such as drug and gene delivery. HAP nanoparticles have been functionalized by various chemicals in order to effectively break down the nanoparticles agglomerates, achieve uniform dispersion in solvent or matrix, form good interfacial bonding with matrix for better composite mechanical properties, and couple with therapeutic molecules. The HAP nanoparticles after grafting with Poly(L-Lactide) (PLA) [37, 38] and Poly(ε-caprolactone) (PCL) [39] can be more uniformly dispersed in the solvent and have better colloidal stability in one step of HAP nanoparticles reinforced (HAP-PLA) composite fabrication. The HAP-PLA nanocomposites containing surface modified HAP nanoparticles have enhanced mechanical properties compared to the composites containing as-fabricated HAP nanoparticles. Shi et al. [40] successfully conjugated the quantum dots with HAP nanoparticles and such nanoparticles exhibited promising luminescent emission *in vitro* and *in vivo*, which may have potential application as biomarkers. In addition, fatty acid (stearic acid)[41], therapeutic molecules[42], pyrophosphoric acid[43], some functional polymers and small organic molecules[44] were also studied to modify the surface of HAP nanoparticles.

In this study, three different carboxylic acid compounds with very similar molecular structure except for one functional group (amine group, carboxyl group, or methyl group) were selected and grafted on HAP nanoparticles to provide different nanoparticles surface charge, while keeping other properties unchanged, in order to systematically investigate the influence of surface charge with minimum interference from other factors. The *in vitro* investigation was conducted using osteoblast cells (MC3T3-E1) and a quantitative evaluation of the effect of surface charge of HAP nanoparticles on cellular uptake and cell proliferation of such cells was carried out.

2. Materials and methods

2.1 Synthesis of HAP nanoparticles

300 ml solution with calcium/phosphorus (Ca/P) ratio of ~1.67 was prepared with 60 mmol (14.17 g, 0.2 mol/L) of $Ca(NO_3)_2{\cdot}4H_2O$ and 36 mmol (5.62 g, 0.12 mol/L) of $NaH_2PO_4{\cdot}2H_2O$ in 300 ml of deionized water. The solution was stirred vigorously and heated to 85 °C and then 300 ml of concentrated ammonium hydroxide solution (28–30% $NH_3{\cdot}H_2O$) was quickly added to the solution, which immediately induced nanoparticle precipitation. The mixture was held at 85 °C for approximately 24 hours to ensure a complete conversion of the starting material to hydroxyapatite. The mixture was then cooled to room temperature and the solid material was settled in the container. Excess liquid was decanted off, and fresh deionized water was added. The mixture was then stirred briefly before allowing the solid to settle and decanting once again. The dilution and decanting process was repeated until the pH value of the mixture was below 9. In this study, these as-fabricated HAP nanoparticles without surface modification are referred as untreated HAP nanoparticles.

2.2 Synthesis of surface modified HAP nanoparticles

The same approach was used as in 2.1 to trigger the nanoparticle precipitation in solution. One minute after adding the ammonium hydroxide solution, which triggered the precipitation, 2.625 mmol (0.0044 mol/L) of the desired carboxylic acid compound (either 12-aminododecanoic acid (0.565 g), dodecanedioic acid (0.604 g), or dodecanoic acid (0.526 g) was added, which could result in amine group, carboxyl group, and methyl group, respectively on the nanoparticle surface. The amount of the carboxylic acid compounds corresponds to 1 mmol of organic compound per 1 gram of hydroxyapatite. The mixture was stirred for additional 15 minutes before being placed in an oven at 95 °C. Once the product was completely dried, it was collected and placed in a centrifuge tube. The product was rinsed with water and the solid was collected by centrifugation. The rinsing and centrifugation were repeated two more times. Next, cyclohexane, replacing water, was used to rinse the solid in the same manner. The rinsed material was again thoroughly dried in an oven at 95 °C.

2.3 Characterization of Nanoparticles

2.3.1 Fourier transform infrared spectroscopy (FT-IR)

Fourier transform infrared spectroscopy (Thermo Nicolet, Madison, Wisconsin, USA) was used to characterize the functional groups of untreated and surface modified HAP nanoparticles. For each spectrum, 16 scans between the wave numbers of 4000 cm^{-1} to 400 cm^{-1} were recorded in the transmission mode by a potassium bromide method.

2.3.2 Zeta potential measurement

Zeta potential of the HAP nanoparticles was determined in phosphate buffered solution (PBS) with pH 7.4 using Zeta meter 3.0+ (Zeta-Meter Inc, Staunton, Virginia, USA).

2.3.3 Powder X-ray diffraction(XRD)

XRD experiments were performed within a 2θ range of 20°-60° on a Scintag Pad V X-ray diffractometer with Cu Kα radiation (1.54 Å) and a Ni filter. Scans of bulk powders were run at 40 kV and 35 mA.

2.3.4 Transmission electron microscopy (TEM)

TEM (JEOL-1400 TEM, USA) was used to investigate the morphology of hydroxyapatite nanoparticles at an acceleration voltage of 100kV.

2.4 Cell culture

Cell studies were performed with the MC3T3-E1 cell line purchased from American Type Culture Collection (Manassas, Virginia, USA). Cells were maintained in modified alpha minimum essential medium (α-MEM) lacking ascorbic acid (AA)(GIBCO), supplemented with 10% fetal bovine serum (FBS) and incubated in a humidified atmosphere at 37 °C and at 5% CO_2. HAP nanoparticles were sterilized in autoclave at 121 °C for 60 minutes before cell culture.

2.4.1 MTT assay—The MTT assay is a simple but very useful tool for evaluating cell vitality and proliferation. The key component is 3-(4,5-dimethylthiazol-2-yl)-2,5-diphenyltetra Zolium bromide (MTT). Mitochondrial dehydrogenases of living cells reduce the tetrazolium ring, yielding a blue formazan product, which can be measured spectro-photometrically. The amount of formazan produced is proportional to the number of viable cells present. For HAP nanoparticles study, cells were lifted with 0.05 wt% trypsin/EDTA(Invitrogen), seeded into 48-well culture plates at 10,000 cells per well with 0.5 ml growth medium, and allowed to attach overnight. The following day, the growth medium in each well was replaced with the medium supplemented with HAP nanoparticles at different concentration or different types of HAP nanoparticles. After 3 more days or 7 more days of culture with HAP nanoparticles, the culture medium in wells was displaced with MTT solution (0.5 mg/ml in α-MEM without FBS). After an incubation of 4 hours at 37 °C, the liquid was aspirated and the insoluble formation produced was dissolved in DMSO/Ethanol (DMSO:Ethanol=1:1) solution. The optical densities were measured at 540nm (Fusion™ alpha microplate analyzer, A Packard BioScience Company).

2.4.2 LDH assay—Lactate dehydrogenase (LDH) activity in the cell medium was determined using a commercial LDH kit (Cayman Chemical Company, Ann Arbor, MI, USA). LDH is a soluble enzyme located in the cytosol. The enzyme is released into the surrounding culture medium upon cell damage or cell lysis, processes that occur during both apoptosis and necrosis. LDH activity, therefore, can be used as an indicator of cell membrane integrity, and thus a measurement of cytotoxicity. One hundred microliters of cell medium was used for LDH analysis. Absorbance was measured at 490 nm (Fusion™ alpha microplate analyzer, A Packard BioScience Company). All the procedures are based on the protocols from the Cayman Chemical Company.

2.4.3 Biological transmission electron microscopy—Briefly, at the end of 3 days incubation, the cells were prefixed with 2 % glutaraldehyde and 2 % paraformaldehyde in 0.1M sodium cacodylate buffer, post-fixed with 1% osmium tetroxide, enbloc stained with 1% aqueous uranyl acetate, dehydrated with a series of alcohols and infiltrated with resin, polymerized with resin in coldspot. The resin samples were thin-sectioned by the Leica Ultracut UCT ultramicrotomes to prepare TEM samples. Then, the TEM samples were investigated by the transmission microscope (JEOL-1400) at an acceleration voltage 100 KV.

2.5 Statistical analysis

Data are presented as the mean ± standard error of mean (SEM) for the indicated number of separate experiments. Statistical analysis of data was performed with one-way analysis of variance (ANOVA) and P-values less than 0.05 were considered significant.

3: Results and discussion

3.1 Modification of HAP nanoparticle surface

In the present study, we intend to evaluate the effect of surface charge on the cellular uptake and biocompatibility of HAP nanoparticles. For systematic study of the surface charges, the surface modification was performed using three different schemes as shown in scheme 1. In reaction class I, the surface hydroxyl groups on HAP reacted with the carboxylic group on 12-aminododecanoic acid and the amine on the other terminal will be protonated in the PBS solution at pH 7.4 to form NH_3^+ with positive charge. In reaction class II, the carboxylic group on dodecanedioic acid reacted with hydroxyl groups to form the HAP nanoparticles with carboxylic group on the surface. The terminal carboxylic group dissociated to proton and COO^- with negative charges in the PBS solution at pH 7.4. For reaction class III, surface hydroxyl groups reacted with carboxylic group on the dodecanoic acid to form the HAP nanoparticles with CH_3 group on the terminal, which can be considered as the neutral HAP nanoparticles in the PBS solution.

Surface modification should be an event occurring only at the HAP surface. Once the state of the bulk properties such as crystallinity and the crystalline phase were changed by the chemical reaction, the as-fabricated HAP nanoparticles may change their intrinsic properties. The XRD patterns in figure 1 indicated that both the untreated nanoparticles and modified nanoparticles have the characteristic peak at 2θ regions of 26°, 29°, 32–34°, 40°, 46–54°, which are consistent with the HAP phase (ICDD 09-432). Our results suggested that the selected reactions are on the HAP surface and the intrinsic properties of HAP, especially the crystalline structure, are maintained.

The transmission electron microscope (TEM) images showed the size distribution and morphology of as-prepared HAP nanoparticles (figure 2). Compared to the untreated HAP nanoparticles, no significant difference on size and morphology was observed on the HAP nanoparticles modified with 12-aminododecanoic acid (positive) and dodecanedioic acid (negative). However, the HAP nanoparticle size increased from 100nm in length, 20nm in diameter to about 150 nm in length and 50 nm in diameter after the surface modification with dodecanoic acid (neutral). Although the reason for the size difference is not very clear, we speculate that dodecanoic acid plays a role in influencing the nucleation and growth of HAP nanoparticles. A different synthesis approach that separates the HAP nanoparticle fabrication from the dodecanoic acid treatment was tried, but it yielded HAP nanoparticles with significant agglomeration with the aggregate size over a few micrometers.

The FT-IR spectroscopy is an effective tool to investigate the functional group on the molecular level. The infrared band of untreated HAP and as-modified HAP nanoparticles are shown in figure 3. The absorption band at about 3570 cm^{-1} represents the stretching vibration mode of lattice OH^-, which was observed in all the samples. The bands at 1090, 1020, 961 cm^{-1} are ascribed to the stretching mode of phosphate, while the bands at 557, 601 and 829 cm^{-1} are characterized as the bending mode of phosphate. The band at 1370 cm^{-1} s shows the carbonate group in the hydroxyapatite structure. Those are all the major characteristic bands of HAP. The broad absorption band from 3600 to 3300 cm^{-1} indicates the existence of the bending mode of absorbed water in the samples. There are very strong absorption bands at 2927 and 2851 cm^{-1} on all the surface modified HAP nanoparticles FT-IR spectroscopy, which are due to the stretching mode of CH_3 or CH_2 groups from the

corresponding fatty acid or derivatives. In addition, all the modified HAP nanoparticles have an absorption band on 1635 cm^{-1}, which can be ascribed to antisymmetric stretching vibration of COOCa from the interaction between COOH and Ca^{2+}. The spectrum of 12-aminododecanoic acid modified HAP nanoparticles(figure 3a) has the two sharp bands at about 3610 cm^{-1}, the stretching mode of amine group (-NH_2), indicative of existence of 12-aminododecanoic acid molecules on the surface of HAP nanoparticles. Moreover, the amine group also exhibits a medium absorption band at 1550 cm^{-1} for bending mode. Besides the above mentioned band, the spectrum in figure 3b (dodecanedioic acid) has a medium absorption band at 1570 cm^{-1}, as evidence of ascribed to the COOH group on the terminal.

Zeta potential measurement was used to determine whether the proposed modifications can generate different surface charged HAP nanoparticles. It can be observed from figure 4, the HAP nanoparticles modified with 12-aminododecanoic (positively charged HAP) has a zeta potential 48.6±5.2mV in the PBS solution at pH 7.4. The untreated HAP nanoparticles, HAP nanoparticles modified with dodecanedioic acid (negatively charged HAP) and dodecanoic acid (neutral HAP) all have the negative zeta potentials, −11.7±0.7mV, −28.3±3.9mV, −11.4±2.5mV, respectively, in PBS solution at pH 7.4. The values for untreated HAP nanoparticles and neutral HAP nanoparticles are consistent with previous studies by other researchers. Tang et al. reported that the zeta potential of HAP nanoparticles become more negative as the size increases; and the zeta potential of HAP nanoparticles with size of 20 nm, 40 nm, and 80 nm are −4.1±0.6 mV, −4.8±0.2 mV and −6.0±1.0 mV, respectively. As shown in figure 1, the length of some HAP nanoparticle is larger than 100 nm, which is probably the reason that untreated HAP and neutral HAP nanoparticles have zeta potential value lower than −6.0 mV. Based on the FT-IR and Zeta potential data, the modifications in scheme 1 were confirmed to work well. For convenience, the 12-aminododecanoic modified, dodecanedioic acid modified and dodecanoic acid modified HAP nanoparticles are referred as positively charged, negatively charged, and neutral HAP nanoparticles, respectively. We use the word “neutral” mainly for simplicity of the description despite of the actual negative charge of these nanoparticles in PBS solution.

3.2 In vitro tests

Cellular uptake is the critical step for the gene delivery and intracellular drug delivery. Many studies have been focused on the cellular uptake behavior and mechanism of nanoparticles. It was believed that shape, size and surface charge influenced the cellular uptake behavior substantially [30, 31, 33, 45]. It was also reported that the positively charged nanoparticles could penetrate into the cells more easily due to the electronic potential of cell membrane is generally known to be negative [6, 14, 30]. The biological TEM images (figure 5a and 5b) showed that many nanoparticles were present in the vacuoles of the grown MC3T3-E1 cells after 3 days incubation in the positively charged HAP nanoparticles medium and their size and morphology were consistent with the HAP nanoparticles. The results of energy dispersive X-ray spectroscopy confirmed that these inorganic particles in the cells have a Ca/P ratio of 1.61. For those negatively charged and untreated HAP nanoparticles MC3T3-E1 cell samples (figure 5c, 5d, 5g, and 5h), some HAP nanoparticles also entered into the vacuole of cells. A careful analysis of the TEM images indicate that the HAP nanoparticles exist in almost all the vacuoles of the cells cultured with positively charged HAP nanoparticles. However, only a small portion of vacuoles have HAP nanoparticles in the cells cultured with the negatively charged and untreated HAP nanoparticles medium. For the neutral HAP nanoparticles with bigger size than the other three samples, no HAP nanoparticle could be observed in the cells from the TEM images (figure 5e and 5f). In summary, positively charged, negatively charged and untreated HAP nanoparticles, with similar size and shape, could be internalized into the MC3T3-E1 cell lines and the amount of uptaken particles for positively charged samples are significantly more than the negatively

charged and untreated samples, while the neutral HAP nanoparticles with bigger size could not be internalized into the MC3T3-E1 cell lines.

Other research results [6, 10] suggested that positively charged silica nanoparticles were easier to be internalized into cells, which are in good agreement with our results. Motskin et al. [31] also studied the uptake of negatively charged HAP nanoparticles of human monocyte-macrophage cells and found that the HAP nanoparticles with higher (less negative) zeta potential value showed greater uptake. Apparently, the zero uptake of neutral nanoparticles in MC3T3-E1 cell could not be explained only based on the hypothesis of influence of surface charge on cellular uptake, as the shape and size may also play a role in cellular uptake. As stated in the previous section (figure 4), the neutral HAP nanoparticles have the size about 150 nm in length and 50 nm in diameter, which is much larger than the corresponding untreated, positively charged and negatively charged HAP nanoparticles with about 100 nm in length and 20 nm in diameter. Gao's receptor-mediate endocytosis study [32] suggest that, for a finite cell membrane, once the size of the particles exceeds the maximum radius, the wrapping process cannot be conducted in terms of the limited number of receptors available to bind. Based on Gao's model, the rod-shape particle has a maximum wrapping size of 320 nm in length, beyond which no receptor-mediated endocytosis process may happen. Although Gao did not include the charge effects in his model, he suggested that negatively charged nanoparticles would have smaller optimal wrapping size as well as smaller maximum wrapping size due to the interaction with the cell membrane with negative charge[32]. The so-called neutral HAP nanoparticle actually has a zeta potential value of −11.4±2.5 mV, which may lead to a maximum wrapping size less than 150 nm in length. This size effect and surface charge effect, combined, might be responsible for the zero uptake of neutral HAP nanoparticles in MC3T3-E1 cells. Considering the untreated and neutral HAP nanoparticles have similar zeta potentials, the bigger size might be the dominant reason for the zero uptake of neutral HAP nanoparticles.

Besides the cellular uptake behavior, the biocompatibility of HAP nanoparticles is also essential to evaluate for the drug delivery, gene delivery and other biomedical applications. To date, no guideline has been presently available to quantify the toxicity effects of nanoparticles. Since HAP is usually used as an artificial substitute material for bone regeneration, in this study, the biocompatibility of HAP nanoparticles was also investigated using the osteoblast (MC3T3-E1 cell lines). The 3 days MTT assay results show that there were almost no significant differences between the control and HAP nanoparticles suspensions except the dosage at 0.5 mg/ml. This phenomenon can be explained by a required induction period for the MC3T3-E1 cell lines to adapt the treatment with HAP nanoparticles before proliferation. After the induction period, MTT assay results showed that exposing cells to HAP nanoparticles for 7 days substantially stimulated cell growth. Most of the previous studies [29, 31, 33–35] showed that HAP nanoparticles penetrated into the cells to cause cell damage and inhibit the cell growth. The inhibiting effect typically increases with high concentration of HAP nanoparticles. Please note that none of the previous studies used MC3T3-E1 cell line and they also used different concentrations. Thus, it is very encouraging to note that the incorporating of HAP nanoparticles can stimulate the cell proliferation. The MTT results in figure 6 also demonstrated that 0.1 mg/ml has the highest absorbance values and at the concentrations of 0.05 mg/ml and 1mg/ml the MC3T3-E1 cells proliferated very well too. In order to study the effect of surface charge on biocompatibility, the concentration of 1 mg/ml was chosen for the following assay.

The 3 days MTT assay results of differently charged HAP nanoparticles (figure 7) shows that the negatively charged and neutral HAP nanoparticles have no significant difference from the control and untreated HAP nanoparticles. During the induction period, cells have to adapt to the calcium phosphate environment. However, the positively charged HAP

nanoparticles can enhance the cell growth very well on 3 days. We hypothesize that the MC3T3-E1 cells cultured with positively charged HAP nanoparticles may have shorter induction period than the cells with other HAP nanoparticles. From the 7 days results, the absorbance values of positively charged HAP nanoparticles are significantly higher than both the control and untreated HAP nanoparticles. Compared to the control, untreated, and neutral charged HAP nanoparticles could stimulate the cell proliferation as well. No significant difference between the control and negatively charged samples was shown on both 3 days and 7 days MTT assay results. It is not clear how the higher cellular uptake of HAP nanoparticles, such as in the case of positively charged HAP nanoparticles, and simply adding HAP nanoparticles in cell culture medium without any cellular uptake, in the case of bigger size neutral HAP nanoparticles, are both related to improved cell proliferation.

The LDH assay is a convenient method to evaluate the cell damage conditions according to the LDH release from cytosol of lysed cells. The 3 days LDH results (figure 8), are consistent with the MTT assay, shows that no significant difference exists on all the samples. After exposure to these nanoparticles for 7 days, it was revealed that the absorbance values of positive, negative and neutral HAP nanoparticles are much lower than the control wells, which means much less damage on cell membrane. Especially for the negatively charged HAP nanoparticles, it is not only significantly lower than the control wells but also having substantial difference with untreated HAP nanoparticles.

Both the MTT and LDH assay results showed that HAP with different dosages and different surface charges can all enhance the cell proliferation and inhibit the cell membrane damage for MC3T3-E1 cell lines, which is a very interesting and desirable phenomenon. From previous studies, the HAP nanoparticles were either toxic to cells or at least inhibit the growth of many cell lines such as microvascular endothelial cells[34], hepatocellular carcinoma cells[46], L929 mouse fibroblasts[35], and osteosarcoma cells[33, 35]. Usually, such results can be explained by two possible mechanisms. Firstly, the uptake of HAP nanoparticles can result in the cell damages and then inhibit the cell proliferation and other properties. Second, the dissolution of HAP nanoparticles will increase the calcium and phosphate concentration either inside or surrounding the cells, which may influence the cellular behavior. In our study, the LDH assay results illustrated that the internalization process of HAP nanoparticles has less cell damage, which may contribute the better biocompatibility. The mechanism about the excellent biocompatibility of the HAP nanoparticle for MC3T3-E1 cells and how uptake of HAP nanoparticles reduced the cell membrane damage will require further systematic investigations.

It is well-known that calcium phosphate is an attractive option for gene delivery in terms of its biodegradability, biocompatibility, convenience of handling and good affinity to pDNA[10, 28, 29]. However, inefficient cellular uptake, which could be attributed to the repulsive force between the negatively charged DNA and cell membrane, is still a key reason for the low level gene expression of calcium phosphate loaded pDNA[28, 47]. From the above results, the positively charged HAP nanoparticles are very promising in the gene delivery application due to its super biocompatibility and higher cellular uptake.

4. Conclusion

In summary, the HAP nanoparticles with different surface charges and different size were synthesized and the influence of such HAP nanoparticles with different surface charges and size on cellular uptake behavior and biocompatibility of MC3T3-E1 cell lines were studied. The HAP nanoparticles with positive charge could be more easily uptaken by the MC3T3-E1 cell lines than other HAP nanoparticles with similar size due to the attractive interaction between positively charged HAP nanoparticles with the negative cell membrane. The size

increase from 100 nm in length and 20 nm in diameter to 150 nm in length and 50 nm in diameter yield zero uptake of HAP nanoparticles. The HAP nanoparticles with different dosage, different charges, and different size could all enhance cell proliferation and result in less cell membrane damage for MC3T3-E1 cell lines. The positively charged HAP nanoparticles have better biocompatibility compared to the other HAP nanoparticles based on MTT and LDH assay. These results provide improved understanding of the influence of surface charge on functional properties of HAP nanoparticles for various biomedical applications, especially for gene delivery and intracellular drug delivery fields.

Acknowledgments

This research was supported by National Institute of Health (1R21DE018821-01A2) and National Science Foundation (CMMI-0846744). The authors wish to acknowledge Mr. Xiaoguang Yang, Ms. Wenwen Sheng, and Ms. Sholpan Askarova for their generous assistance and meaningful discussion during the research.

References

1. Fayazpour F, Lucas B, Alvarez-Lorenzo C, Sanders NN, Demeester J, De Smedt SC. Physicochemical and transfection properties of cationic hydroxyethylcellulose/DNA nanoparticles. Biomacromolecules. 2006; 7:2856–62. [PubMed: 17025362]
2. Cai YR, Pan HH, Xu XR, Hu QH, Li L, Tang RK. Ultrasonic controlled morphology transformation of hollow calcium phosphate nanospheres: A smart and biocompatible drug release system. Chemistry of Materials. 2007; 19:3081–3.
3. Yang PP, Quan ZW, Lu LL, Huang SS, Lin J. Luminescence functionalization of mesoporous silica with different morphologies and applications as drug delivery systems. Biomaterials. 2008; 29:692–702. [PubMed: 17996294]
4. Wilhelm C, Gazeau F. Universal cell labelling with anionic magnetic nanoparticles. Biomaterials. 2008; 29:3161–74. [PubMed: 18455232]
5. Chlopek J, Czajkowska B, Szaraniec B, Frackowiak E, Szostak K, Beguin F. In vitro studies of carbon nanotubes biocompatibility. Carbon. 2006; 44:1106–11.
6. Chung TH, Wu SH, Yao M, Lu CW, Lin YS, Hung Y, Mou CY, Chen YC, Huang DM. The effect of surface charge on the uptake and biological function of mesoporous silica nanoparticles 3T3-L1 cells and human mesenchymal stem cells. Biomaterials. 2007; 28:2959–66. [PubMed: 17397919]
7. Tang YJJ, Ashcroft JM, Chen D, Min GW, Kim CH, Murkhejee B, Larabell C, Keasling JD, Chen FQF. Charge-associated effects of fullerene derivatives on microbial structural integrity and central metabolism. Nano Letters. 2007; 7:754–60. [PubMed: 17288489]
8. Sayes CM, Gobin AM, Ausman KD, Mendez J, West JL, Colvin VL. Nano-C-60 cytotoxicity is due to lipid peroxidation. Biomaterials. 2005; 26:7587–95. [PubMed: 16005959]
9. Wan SR, Huang JS, Guo M, Zhang HK, Cao YJ, Yan HS, Liu KL. Biocompatible superparamagnetic iron oxide nanoparticle dispersions stabilized with poly(ethylene glycol)oligo(aspartic acid) hybrids. Journal of Biomedical Materials Research Part A. 2007; 80A: 946–54. [PubMed: 17083116]
10. Tan K, Cheang P, Ho IAW, Lam PYP, Hui KM. Nanosized bioceramic particles could function as efficient gene delivery vehicles with target specificity for the spleen. Gene Ther. 2007; 14:828–35. [PubMed: 17344903]
11. Nimesh S, Chandra R. Polyethylenimine nanoparticles as an efficient in vitro siRNA delivery system. European Journal of Pharmaceutics and Biopharmaceutics. 2009; 73:43–9. [PubMed: 19362592]
12. Woitiski CB, Neufeld RJ, Ribeiro AJ, Veiga F. Colloidal carrier integrating biomaterials for oral insulin delivery: Influence of component formulation on physicochemical and biological parameters. Acta Biomaterialia. 2009; 5:2475–84. [PubMed: 19362890]
13. Acharya S, Dilnawaz F, Sahoo SK. Targeted epidermal growth factor receptor nanoparticle bioconjugates for breast cancer therapy. Biomaterials. 2009; 30:5737–50. [PubMed: 19631377]

14. Thomas C, Gupta V, Ahsan F. Influence of surface charge of PLGA particles of recombinant hepatitis B surface antigen in enhancing systemic and mucosal immune responses. International Journal of Pharmaceutics. 2009; 379:41–50. [PubMed: 19524654]
15. Zhou J, Moya S, Ma L, Gao C, Shen J. Polyelectrolyte Coated PLGA Nanoparticles: Templation and Release Behavior. Macromolecular Bioscience. 2009; 9:326–35. [PubMed: 19089871]
16. Perrault SD, Walkey C, Jennings T, Fischer HC, Chan WCW. Mediating Tumor Targeting Efficiency of Nanoparticles Through Design. Nano Letters. 2009; 9:1909–15. [PubMed: 19344179]
17. Kamei K, Mukai Y, Kojima H, Yoshikawa T, Yoshikawa M, Kiyohara G, Yamamoto TA, Yoshioka Y, Okada N, Seino S, Nakagawa S. Direct cell entry of gold/iron-oxide magnetic nanoparticles in adenovirus mediated gene delivery. Biomaterials. 2009; 30:1809–14. [PubMed: 19136151]
18. Li D, He Q, Li J. Smart core/shell nanocomposites: Intelligent polymers modified gold nanoparticles. Advances in Colloid and Interface Science. 2009; 149:28–38. [PubMed: 19201389]
19. Teja AS, Koh P-Y. Synthesis, properties, and applications of magnetic iron oxide nanoparticles. Progress in Crystal Growth and Characterization of Materials. 55:22–45.
20. Yu F, Huang Y, Cole AJ, Yang VC. The artificial peroxidase activity of magnetic iron oxide nanoparticles and its application to glucose detection. Biomaterials. 2009; 30:4716–22. [PubMed: 19515418]
21. Cauda V, Schlossbauer A, Kecht J, Zurner A, Bein T. Multiple Core-hell Functionalized Colloidal Mesoporous Silica Nanoparticles. Journal of the American Chemical Society. 2009; 131:11361–70. [PubMed: 19722649]
22. Cauda V, Schlossbauer A, Kecht J, Zurner A, Bein T. Multiple Core-shell Functionalized Colloidal Mesoporous Silica Nanoparticles. Journal of the American Chemical Society. 2009; 131:11361–70. [PubMed: 19722649]
23. Arcis RW, Lopez-Macipe A, Toledano M, Osorio E, Rodriguez-Clemente R, Murtra J, Fanovich MA, Pascual CD. Mechanical properties of visible light-cured resins reinforced with hydroxyapatite for dental restoration. Dental Materials. 2002; 18:49–57. [PubMed: 11740964]
24. Hile, David D.; Doherty, Stephen A.; Trantolo, Debra J. Prediction of resorption rates for composite polylactide/hydroxylapatite internal fixation devices based on initial degradation profiles. Journal of Biomedical Materials Research Part B: Applied Biomaterials. 2004; 71B:201–5.
25. Hasegawa S, Ishii S, Tamura J, Furukawa T, Neo M, Matsusue Y, Shikinami Y, Okuno M, Nakamura T. A 5–7 year in vivo study of high-strength hydroxyapatite/poly(l-lactide) composite rods for the internal fixation of bone fractures. Biomaterials. 2006; 27:1327–32. [PubMed: 16213581]
26. Rameshbabu N, Kumar TSS, Prabhakar TG, Sastry VS, Murty KVGK, Rao KP. Antibacterial nanosized silver substituted hydroxyapatite: Synthesis and characterization. Journal of Biomedical Materials Research Part A. 2007; 80A:581–91. [PubMed: 17031822]
27. Palazzo B, Iafisco M, Laforgia M, Margiotta N, Natile G, Bianchi C, Walsh D, Mann S, Roveri N. Biomimetic Hydroxyapatite-Drug Nanocrystals as Potential Bone Substitutes with Antitumor Drug Delivery Properties. Advanced Functional Materials. 2007; 17:2180–8.
28. Olton D, Li J, Wilson ME, Rogers T, Close J, Huang L, Kumta PN, Sfeir C. Nanostructured calcium phosphates (NanoCaPs) for non-viral gene delivery: Influence of the synthesis parameters on transfection efficiency. Biomaterials. 2007; 28:1267–79. [PubMed: 17123600]
29. Zhu SH, Huang BY, Zhou KC, Huang SP, Liu F, Li YM, Xue G, Long ZG. Hydroxyapatite nanoparticles as a novel gene carrier. Journal of Nanoparticle Research. 2004; 6:307–11.
30. Ling, HuZM.; Changyou, Gao. Colloidal particles for cellular uptake and delivery. Journal of Materials Chemistry. 2009; 19
31. Motskin M, Wright DM, Muller K, Kyle N, Gard TG, Porter AE, Skepper JN. Hydroxyapatite nano and microparticles: Correlation of particle properties with cytotoxicity and biostability. Biomaterials. 2009; 30:3307–17. [PubMed: 19304317]
32. Huajian Gao WS, Freund Lambert B. Mechanics of receptor-mediated endocytosis. PNAS. 2005; 102:9469–74. [PubMed: 15972807]

33. Cai YR, Liu YK, Yan WQ, Hu QH, Tao JH, Zhang M, Shi ZL, Tang RK. Role of hydroxyapatite nanoparticle size in bone cell proliferation. Journal of Materials Chemistry. 2007; 17:3780–7.
34. Pezzatini S, Solito R, Morbidelli L, Lamponi S, Boanini E, Bigi A, Ziche M. The effect of hydroxyapatite nanocrystals on microvascular endothelial cell viability and functions. Journal of Biomedical Materials Research Part A. 2006; 76A:656–63. [PubMed: 16294324]
35. Qiang Fu MNR, Zhou Nai, Huang Wenhai, Wang Deping, Zhang Liying, Li Haifeng. In vitro study on different cell response to spherical hydroxyapatite nanoparticles. Journal of Biomaterials Applications. 2008; 23:37–51. [PubMed: 18194997]
36. Zhao Y, Zhang Y, Ning F, Guo D, Xu Z. Synthesis and cellular biocompatibility of two kinds of HAP with different nanocrystal morphology. Journal of Biomedical Materials Research Part B: Applied Biomaterials. 2007; 83B:121–6.
37. Hong Z, Zhang P, He C, Qiu X, Liu A, Chen L, Chen X, Jing X. Nano-composite of poly(l-lactide) and surface grafted hydroxyapatite: Mechanical properties and biocompatibility. Biomaterials. 2005; 26:6296–304. [PubMed: 15913758]
38. Hong Z, Qiu X, Sun J, Deng M, Chen X, Jing X. Grafting polymerization of L-lactide on the surface of hydroxyapatite nano-crystals. Polymer. 2004; 45:6699–706.
39. Lee HJ, Choi HW, Kim KJ, Lee SC. Modification of Hydroxyapatite Nanosurfaces for Enhanced Colloidal Stability and Improved Interfacial Adhesion in Nanocomposites. Chemistry of Materials. 2006; 18:5111–8.
40. Yan Guo DS, Lian Jie, Dong Zhongyun, Wang Wei, Cho Hoonsung, Liu Guokui, Wang Lumin, Ewing Rodney C. Quantum dot conjugated hydroxyapatite nanoparticles for in vivo imaging. Nanotechnology. 2008; 19:175102.
41. Li Y, Weng W. Surface modification of hydroxyapatite by stearic acid: characterization and in vitro behaviors. Journal of Materials Science: Materials in Medicine. 2008; 19:19–25. [PubMed: 17569011]
42. Murugan R, Ramakrishna S. Coupling of therapeutic molecules onto surface modified coralline hydroxyapatite. Biomaterials. 2004; 25:3073–80. [PubMed: 14967541]
43. Tanaka H, Futaoka M, Hino R, Kandori K, Ishikawa T. Structure of synthetic calcium hydroxyapatite particles modified with pyrophosphoric acid. Journal of Colloid and Interface Science. 2005; 283:609–12. [PubMed: 15721940]
44. Liu Q, Wijn JRd, Blitterswijk CAv. A study on the grafting reaction of isocyanates with hydroxyapatite particles. Journal of Biomedical Materials Research. 1998; 40:358–64. [PubMed: 9570065]
45. Stephanie EA, Gratton PAR, Pohlhans Patrick D, Christopher J, Luft, Madden Victoria J, Napier Mary E, Desimone Joseph M. The effect of particle design on cellular internalization pathways. PNAS. 2008; 105:11613–8. [PubMed: 18697944]
46. Meizhen Yin YH, Bauer Ingo W, Chen Pei, Li Shipu. Effect of hydroxyapatite nanoparticles on the ultrastructure and function of hepatocellular caricinoma cells in vitro. Biomedical Materials. 2006; 1:38–41. [PubMed: 18458384]
47. Dan Luo a WMS. Synthetic DNA delivery systems. Nature Biotechnology. 2000; 18:33–7.

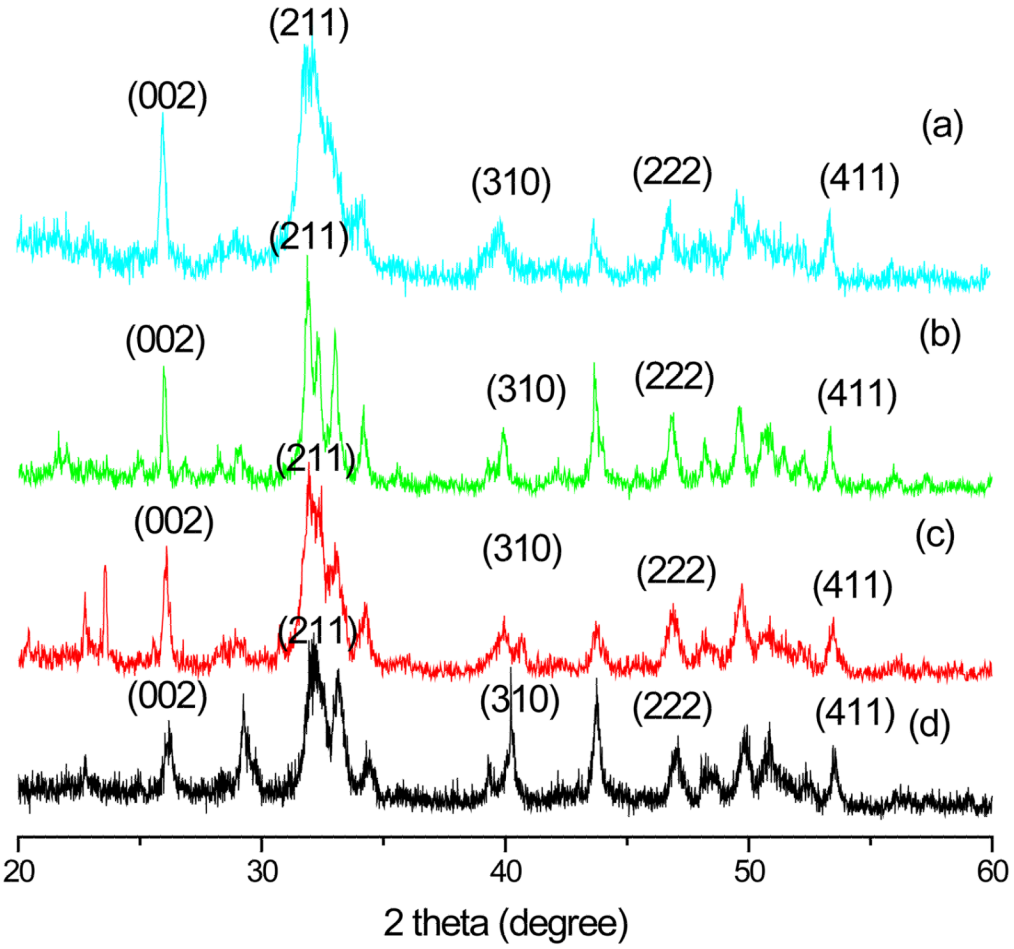

Figure 1.
XRD patterns of (a) 12-aminododecanoic modified HAP nanoparticles, (b) dodecanedioic acid modified HAP nanoparticles, (c) dodecanoic acid modified HAP nanoparticles, and (d) untreated HAP nanoparticles.

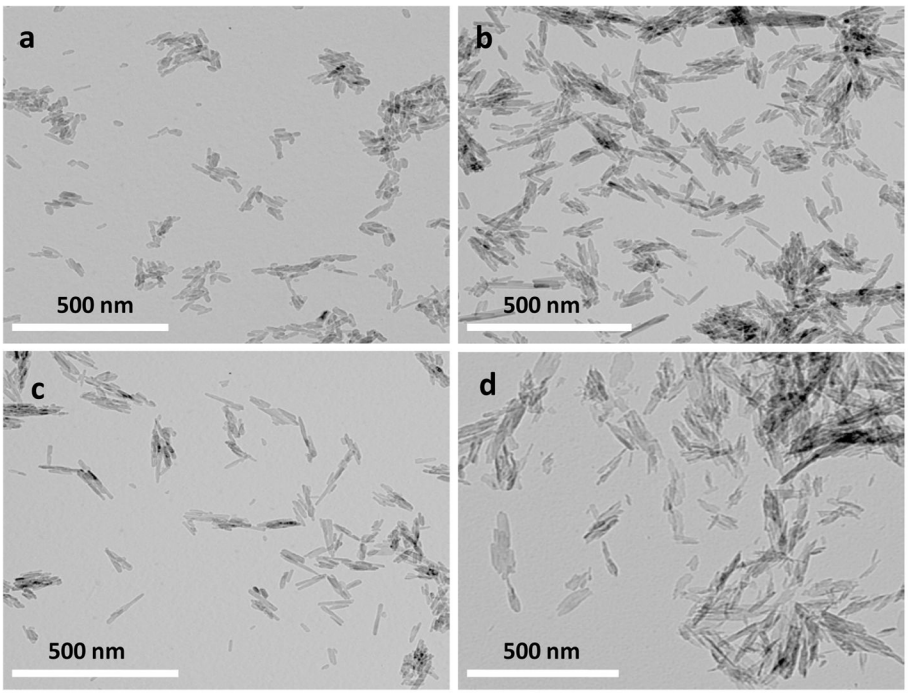

Figure 2.
The TEM images of HAP nanoparticles: (a) untreated, (b) 12- aminododecanoic acid modified, (c) dodecanedioic acid modified, (d) dodecanoic acid modified.

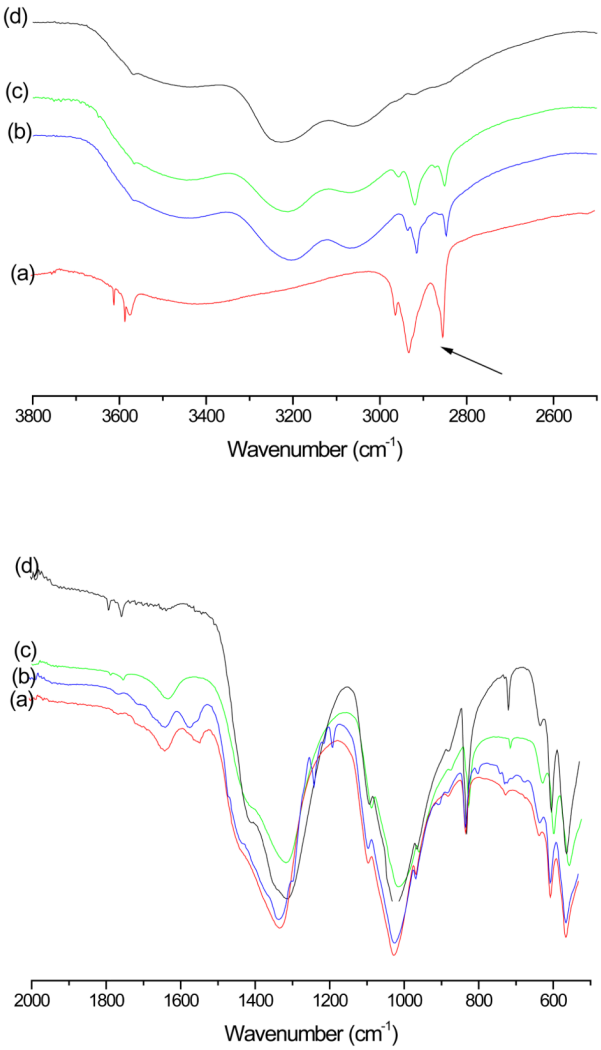

Figure 3.
The FT-IR spectra of HAP nanoparticles treated with (a) 12-aminododecanoic acid, (b) dodecanedioic acid, and (c) dodecanoic acid, and (d) untreated HAP nanoparticles.

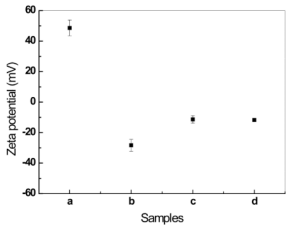

Figure 4.
Zeta potentials of the HAP nanoparticles: (a) 12-aminododecanoic modified, (b) dodecanedioic acid modified, (c) dodecanoic acid modified, (d) untreated, in PBS solution at pH value of 7.4.

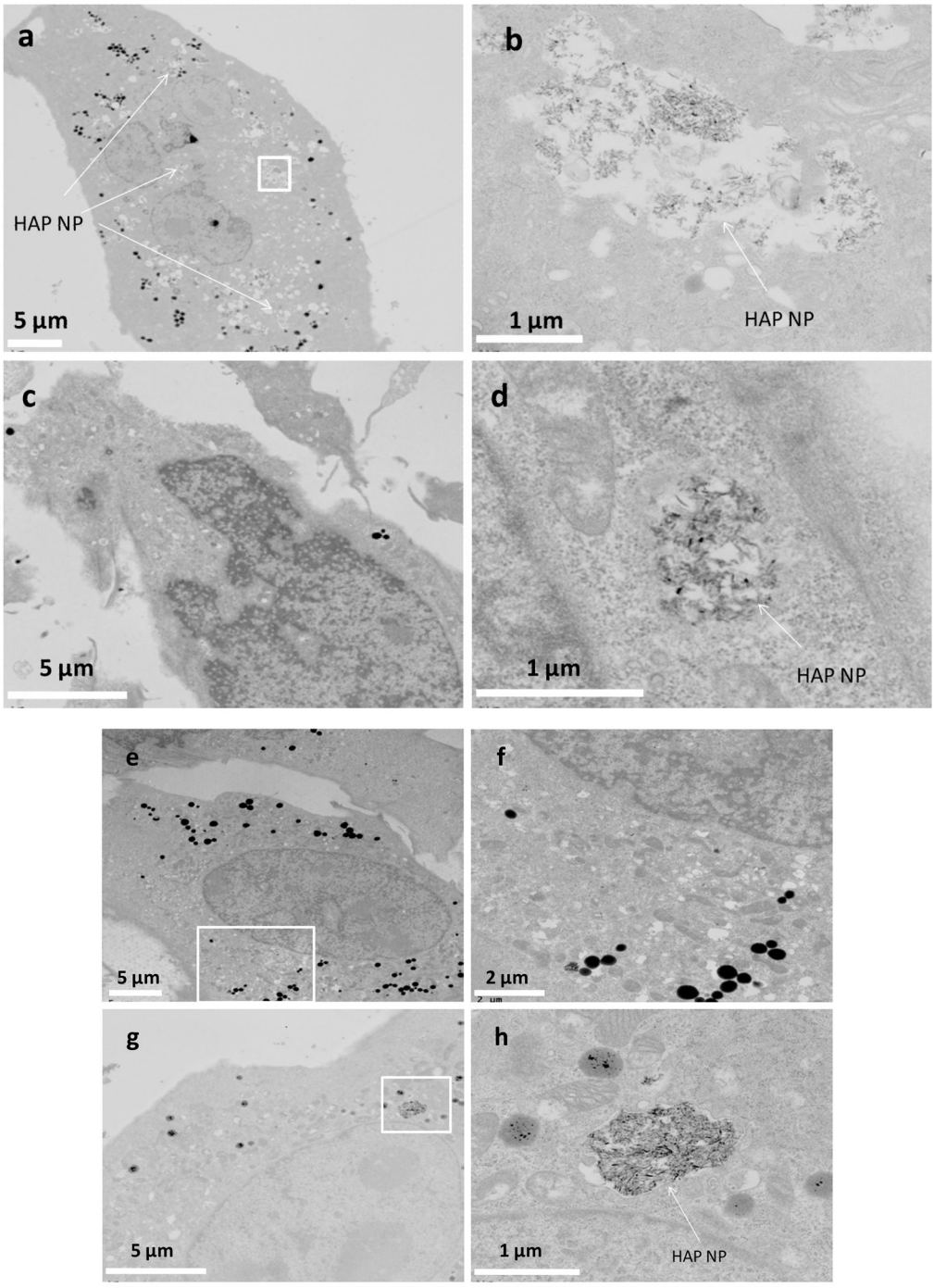

Figure 5.
The TEM images of MC3T3-E1 cell lines cultured in medium with different HAP nanoparticles for 3days: (a, b) positively charged HAP nanoparticles, (c, d) negatively charged HAP nanoparticles, (e, f) neutral HAP nanoparticles, (g, h) untreated HAP nanoparticles. The TEM images on the right are the enlargement of rectangle area on the corresponding images on the left side.

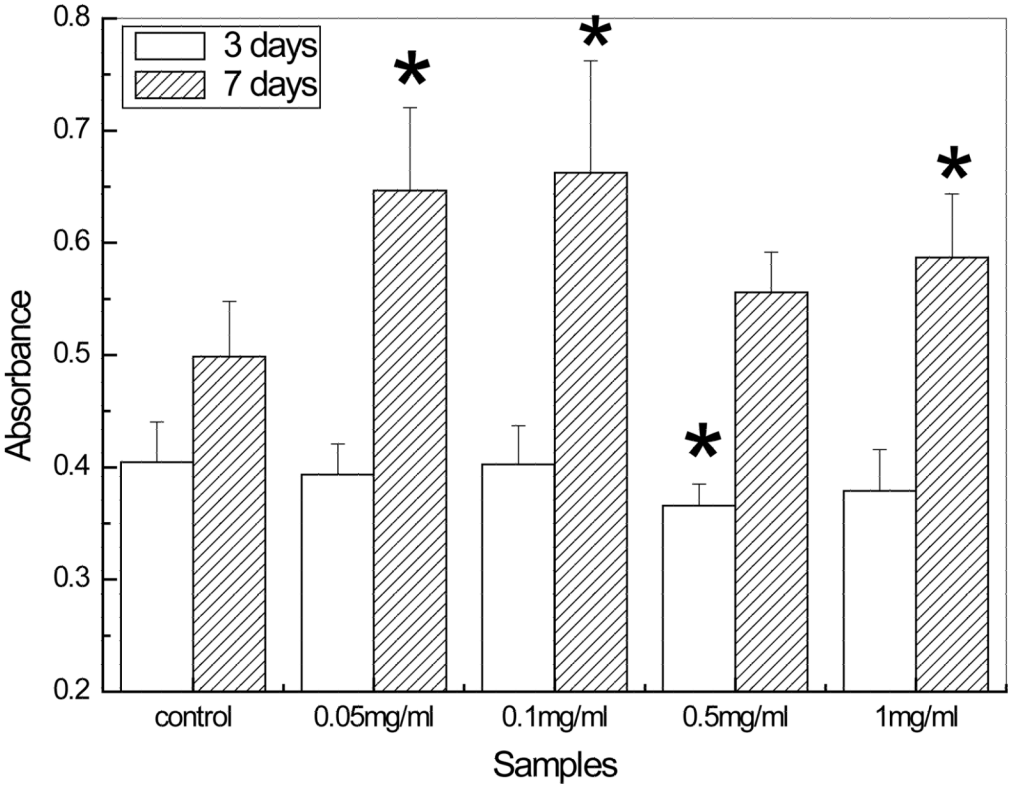

Figure 6.
The proliferation of MC3T3-E1 cell lines on different dosages of untreated HAP nanoparticles by MTT assay. The polystyrene well without hydroxyapatite nanoparticles was used as the control. Data are presented as the average±SD for n=5. *indicate $P<0.05$ relative to controls.

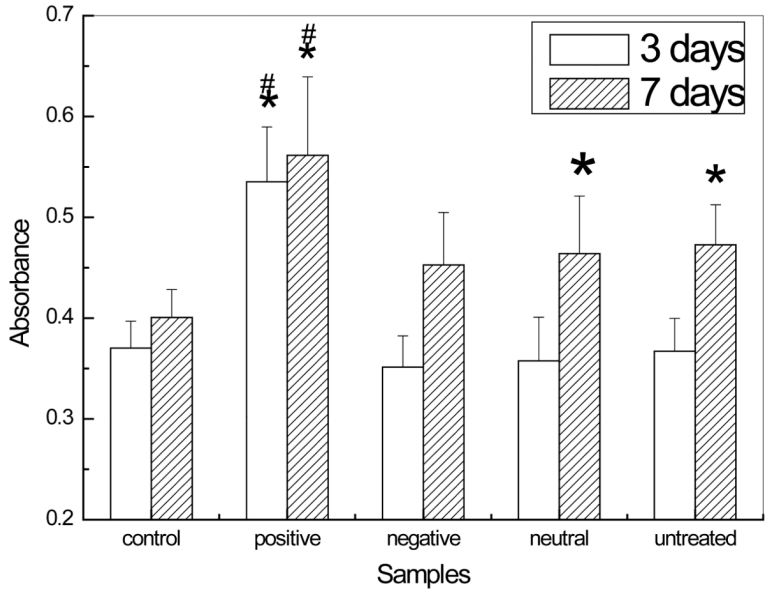

Figure 7.

The proliferation of MC3T3-E1 cell lines on differently charged HAP nanoparticles with dosage 1 mg/ml by MTT assay. The polystyrene well without hydroxyapatite nanoparticles was used as the control. Data are presented as the average±SD for n=5. *indicate $P<0.05$ relative to controls, # indicate $P<0.05$ relative to untreated HAP nanoparticles.

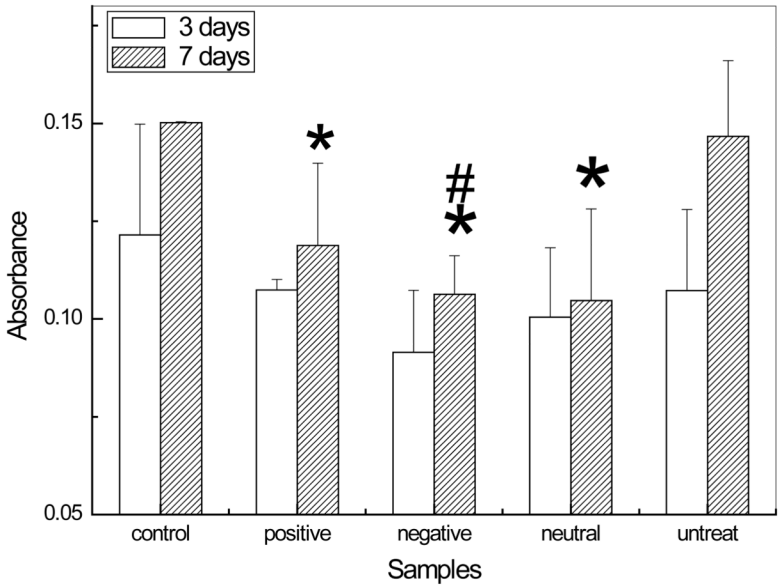

Figure 8.

The LDH activities in the cell culture medium after 3 or 7 days exposure to the differently charged HAP nanoparticles on the dosage of 1mg/ml. The polystyrene well without hydroxyapatite nanoparticles was used as the control. Data are presented as the average±SD for n=5. *indicate $P<0.05$ relative to controls, # indicate $P<0.05$ relative to untreated HAP nanoparticles.

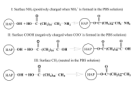

Scheme 1.
Reaction routes for surface modification on HAP nanoparticles.